Regenerative Therapy 16 (2021) 32–41

Contents lists available at ScienceDirect

Regenerative Therapy

journal homepage: http://www.elsevier.com/locate/reth

Original Article

Development of a nasal mucosa-removal model for evaluating cell therapy

Shun Kikuchi [a, b], Tsunetaro Morino [a, b], Ryo Takagi [a], Otori Nobuyoshi [b], Hiromi Kojima [b], Masayuki Yamato [a, *]

[a] Institute of Advanced Biomedical Engineering and Science, Tokyo Women's Medical University, Tokyo, Japan
[b] Department of Otorhinolaryngology, Jikei University School of Medicine, Tokyo, Japan

ARTICLE INFO

Article history:
Received 2 November 2020
Received in revised form
26 November 2020
Accepted 23 December 2020

Keywords:
Animal models
Bone hyperplasia
Cell sheet transplantation
Chronic rhinosinusitis
Maxillary sinus
Nasal mucosa regeneration

ABSTRACT

Introduction: Endoscopic sinus surgery is an effective surgical procedure for treating chronic sinusitis; however, extensive exposure of the bone in the nasal cavity can result in permanent disability post-operatively. Particularly, closure of the sinus drainage pathway due to bone hyperplasia associated with bone exposure can trigger the recurrence of sinusitis. It is essential to regenerate the nasal mucosa after surgery to avoid bone hyperplasia. Regenerative medicine, including cell therapy, could be one of the leading options for nasal mucosa regeneration. To date, there is a lack of effective models for evaluating treatments for prevention of bone hyperplasia that occurs after sinus surgery. The purpose of this study was to develop a model of nasal mucosal removal to evaluate cellular therapies.

Methods: The model was created in rabbits, a species with a wide nasal structure, and was generated by approaching the maxillary sinus from the nasal bone side and solely removing the maxillary sinus mucosa without destroying the structures in the nasal cavity. Adipose-derived mesenchymal stromal cell sheets prepared in temperature-responsive cell culture dishes were examined for the effect of transplantation in the animal model. Intranasal evaluation was assessed by micro-computed tomography and tissue staining.

Results: Significant bone hyperplasia in the maxillary sinus occurred on the side of mucosal removal, and no bone hyperplasia occurred in the control sham side in the same rabbits on postoperative day 28. Bone hyperplasia was observed over a short time period, with the presence of bone hyperplasia in the maxillary sinus on day 14 and calcification of the bone on day 28. The adipose-derived mesenchymal stromal cell (ADSC) sheet was transplantable in a nasal mucosa-removal model. No significant differences in bone hyperplasia were found between the transplantation side and the sham side in terms of the effect of transplantation of the ADSC sheet; however, bone hyperplasia tended to be suppressed on the transplantation side.

Conclusions: This animal model is simple, highly reproducible, and does not require special equipment or drugs. In addition, this model can be used for various therapeutic interventions, including cell therapy. The presence or absence of the nasal mucosa affects bone remodeling, which highlights the importance of regeneration of the nasal mucosa. In the nasal mucosal regeneration therapy, the ADSC sheet had an inhibitory effect on bone hyperplasia. The nasal mucosa-removal model allows observation of conditions associated with nasal mucosa removal and evaluation of the effectiveness of cell therapy.

Abbreviations: ADSC, adipose-derived mesenchymal stromal cell; EDTA, ethylenediaminetetraacetic acid; HE, hematoxylin and eosin; micro-CT, Micro-computed tomography; PBS, phosphate-buffered saline; POD, postoperative day; SEM, standard error of the mean; SPF, specific-pathogen-free.

* Corresponding author. Institute of Advanced Biomedical Engineering and Science, Tokyo Women's Medical University, 8-1 Kawada-cho, Shinjuku-ku, Tokyo, Japan. Fax: +81- 3-3359-6046.

E-mail addresses: kikuchient@jikei.ac.jp (S. Kikuchi), morino.tsunetaro@twmu.ac.jp (T. Morino), takagi.ryo@twmu.ac.jp (R. Takagi), otori@jikei.ac.jp (O. Nobuyoshi), kojimah@jikei.ac.jp (H. Kojima), yamato.masayuki@twmu.ac.jp (M. Yamato).

Peer review under responsibility of the Japanese Society for Regenerative Medicine.

https://doi.org/10.1016/j.reth.2020.12.004

1. Introduction

Chronic rhinosinusitis is one of the most common diseases in rhinology. Treatment of chronic rhinosinusitis involves drug therapy or surgery; the latter is performed for chronic sinusitis that cannot be controlled with medication. Surgery for chronic rhinosinusitis, especially chronic rhinosinusitis with nasal polyps, is performed globally. Indications for endoscopic sinus surgery have expanded to include endoscopic modified Lothrop procedure [1, 2, 3] and skull base surgery [4, 5, 6] which are difficult to perform without removing the mucosa. The flap procedure of the nasal mucosa, which covers the exposed bone surface to prevent bone hyperplasia in endoscopic sinus surgery, is commonly performed. When the bone is extensively exposed, it is difficult for the flap to cover the entire bone. Moreover, the frap technique exposes the bone in a different location. In addition, in endoscopic sinus surgery for chronic sinusitis, removing the diseased mucous is considered necessary; however, removing the entire nasal mucosa results in poor mucosal regeneration. When bone hyperplasia occurs in the drainage pathway (especially the frontal sinus drainage pathway) with mucosal removal, rhinosinusitis recurs, and this condition is highly refractory. There is a reported success in regenerating the middle ear mucosa by transplanting nasal mucosal epithelial cell sheet into a rabbit middle ear mucosa-removal model [7]. This has been successfully clinically applied in humans as well [8]. There is no effective way to regenerate the nasal mucosa, including treatments such as medications or wound dressings. However, regenerative medicine including cell therapy and cell sheets is expected to be the most efficient method of regenerating the nasal mucosa.

Remodeling of the maxilla has been extensively studied in dentistry [9, 10]. In particular, bone hyperplasia in the maxillary sinus has been extensively studied in sinus floor elevation [11–13]. Animal models are useful for the analysis of the pathogenesis of bone hyperplasia in the nasal cavity and to evaluate treatments. However, there is a lack of pathological models in which the nasal mucosa has been removed, which resembles the procedure performed in human surgery.

Critical aspects of animal models include ease of manipulation, high reproducibility, and ease of evaluation. Moreover, preclinical therapeutic development requires animal models that can be used for various therapeutic interventions. In the present study, we developed an animal model of bone hyperplasia in the maxillary sinus by removing the nasal mucosa. This model is simple, reproducible, and allows for the investigation of efficacy of regenerative medicine, including cell transplantation.

2. Methods

2.1. Animals

All experimental protocols were approved by the animal welfare committee of the Tokyo Women's Medical University (approval number: AE19-010,2019). Male New Zealand White non-specific-pathogen-free (SPF) rabbits (approximate weight, 3000 g) were purchased from the Japan Laboratory Animals (Tokyo, Japan), and male New Zealand White SPF rabbits (approximate weight, 3000 g) were purchased from the Kitayama Labes (Nagano, Japan). Rabbits were injected intramuscularly with 0.7–2.0 mg/kg midazolam (Astellas, Tokyo, Japan), 0.17–0.5 mg/kg butorphanol (Meiji Seika Pharma, Tokyo, Japan), and 0.17–0.5 mg/kg medetomidine (Zenoaq, Tokyo, Japan) for anesthesia. The rabbits were placed in a prone position 15 min after injection to develop the nasal mucosa-removal model and adipose-derived mesenchymal stromal cell (ADSC) sheet transplantation model, and in a supine position during inguinal fat collection. The rabbits were injected intramuscularly for deep anesthesia with 130 mg/kg pentobarbital sodium (Kyoritsu Seiyaku Corporation, Tokyo, Japan) for sacrifice.

2.2. Nasal mucosa-removal model in rabbits

Body hairs above the nose were shaved. A skin incision was made approximately 5 cm above the median line of the nasal bone from the top of the head to the nasal apex, and the skin flap was deployed on both sides. A drilling point of the nasal bone was made. The apex of the nose to the inner corner of the eye at a ratio of 5:3 was opened by 5–8 mm using a diamond bar drill (XPS Micro Resector console Model 2000, Xomed Surgical Products, Florida, USA) (Fig. 1a). The anterior and superior maxillary mucosa was removed. As the connection between the nasal mucosa and maxillary sinus bone is weak, the nasal mucosa could be removed in a single clump extrication using Hartmann Ear forceps (Spiggle & Theis, Overath, Germany) without special operations under a microscope (SN-100(T), Nagashima Medical Inst, Tokyo, Japan) and endoscopy (TESALA, AVS, Tokyo, Japan) (Fig. 1b and c). The control sham side underwent fenestration of the nasal bone without mucosal removal. The hole in the nasal bone was covered with silicone (Exafine putty type, GC corporation, Tokyo, Japan) (Fig. 1d). The skin incision was sutured using nylon thread.

2.3. Micro-computed tomography imaging

Micro-computed tomography (micro-CT) was performed using R_mCT2 (Rigaku, Tokyo, Japan) at 1, 3, 7, 14, and 28 days after sacrifice. The rabbits were scanned using micro-CT with an X-ray source of 90 kV/160 μA with a field of view of 60 mm × 60 mm.

2.4. Measurement of the maxillary sinus bone area

Micro-CT images were analyzed by adjusting the axis with Osirix (OsiriX MD software, version 11.0). In the coronal sections, the point of intersection of the superior part of the maxillary sinus and the inferior part of the maxillary sinus was defined as the middle area. The 2 mm anterior position in the middle area was defined as the anterior area. The 2 mm posterior position in the middle area was defined as the posterior area. ImageJ software (National Institutes of Health, Bethesda, MD, USA) was used to calculate the maxillary sinus bone area.

2.5. Tissue preparation and immunohistochemistry

The rabbits were decapitated using a scalpel and scissors, and the head skin was peeled off. The trimmed head was cut perpendicular to the nose bone approximately every 5 mm using an electric saw (K-100 Bandsaw, Hozan Tool IND, Osaka, Japan). Specimens were fixed in 4% paraformaldehyde for 1–2 days, followed by decalcification in ethylenediaminetetraacetic acid (EDTA)-2Na for 4–8 weeks. After decalcification, specimens were embedded in paraffin (Tissue-TekVIP6; Sakura Finetek, Tokyo, Japan), and then serial coronal sections (5 μm thick for paraffin sections) were cut and mounted on PLATINUM PRO adhesive glass slides (Matsunami Glass, Osaka, Japan). For cross-sectional observations, hematoxylin and eosin (HE) staining was performed using conventional methods. First, Paraffin sections were deparaffinized, rehydrated, and incubated with proteinase K (S3020; Dako, Tokyo, Japan) for antigen retrieval. All sections were incubated with peroxidase-blocking solution (S2030; Dako, Tokyo, Japan) and a blocking reagent (Blocking One Histo; Nacalai Tesque, Kyoto, Japan) to reduce nonspecific antibody binding. Second, the paraffin sections were incubated with mouse monoclonal anti-pan-cytokeratin primary antibody (1:100 dilution, AE1/AE3; Abcam, Tokyo, Japan).

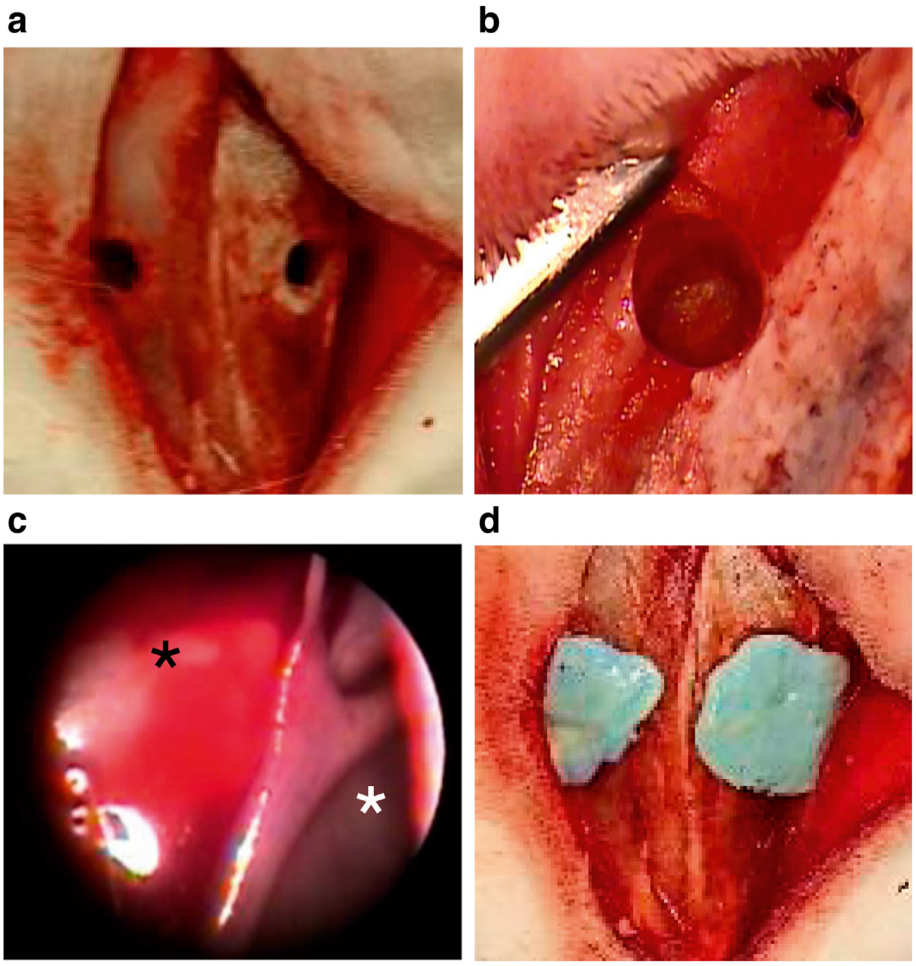

Fig. 1. The nasal mucosa removal model in rabbits. (a) After an incision was made in the middle line of the nasal bone, the lateral nasal bones on both sides were opened by drilling. (b) Microscopic view showing opening of the nasal bone. (c) Endoscopic view showing the maxillary sinus. White and black asterisks indicate the presence of normal nasal mucosa and the area of nasal mucosa removed, respectively. (d) Closure of the hole with silicon.

Third, the paraffin sections were antigen-activated using heat treatment (125 °C for 30 s and 90 °C for 10 s) and incubated with a mouse monoclonal anti-vimentin primary antibody (1:100 dilution, M0725; Dako, Tokyo, Japan). Forth, the paraffin sections were incubated with a horseradish peroxidase-conjugated secondary antibody (EnVision Detection Systems, Peroxidase/DAB, Mouse; Dako, Tokyo, Japan). Fifth, The paraffin sections were incubated with 3,3′-diaminobenzidine solution (DAB; Dako, Tokyo, Japan) for approximately 1 min. Nuclear staining for immunohistochemistry was performed using hematoxylin.

2.6. Isolation and culture of ADSCs

ADSCs were isolated from inguinal fat using a previously reported method with modifications [14]. Briefly, inguinal fat was enzymatically digested with 0.1% type-2 collagenase (Worthington Biochemical Corporation, Lakewood, NJ, USA) at 37 °C for 1 h under shaking. The stromal vascular fraction was extracted after centrifugation for 5 min at 2000 rpm. Cells in the interstitial vascular fraction were cultured in complete culture medium (DMEM; Fujifilm Wako Pure Chemical Corporation, Osaka, Japan) containing 10% fetal bovine serum (FBS; Life Technologies, Frederick, MD, USA) and 1% penicillin/streptomycin (Fujifilm Wako Pure Chemical Corporation, Osaka, Japan) at 37 °C under a 5% CO_2 atmosphere. The medium was changed every 1–2 days. The cells were passaged every 3–5 days using trypsin–EDTA (Fujifilm Wako Pure Chemical Corporation, Osaka, Japan) and plated at a density of 1×10^5 cells/dish. Cells at passage 5 were used in this study. All ADSCs were obtained from one rabbit.

2.7. Flow cytometry assay

A total of 1 000 000 cells were suspended in 100 mL phosphate-buffered saline (PBS) containing 10 mg/mL of each specific antibody. The following primary antibodies were used to detect surface markers: mouse monoclonal anti-CD44 (MCA806GA, BIORAD, California, USA), rat monoclonal anti-CD73 (25073180, Fisher Scientific, New Hampshire, USA), mouse monoclonal anti-CD90 (554895, BD Biosciences, New Jersey, USA), mouse monoclonal anti-CD31 (NB600-562, Funakoshi, Tokyo, Japan), rat monoclonal anti-CD34 (GTX28158, Gene Tex, California, USA), and mouse monoclonal anti-CD45 (MCA808GA, BIORAD, California, USA). After incubation for 60 min at 4 °C, the cells were washed with PBS, and goat anti-mouse IgG H&L (fluorescein isothiocyanate) secondary antibodies (ab6785) were used to detect primary antibodies. After incubation for 60 min at 4 °C, the cells were washed with PBS and then suspended in 0.5 mL PBS for analysis. Cell fluorescence was determined using a Gallios flow cytometer (Beckman Coulter, Tokyo, Japan). Data were analyzed using Kaluza software (Beckman Coulter, Tokyo, Japan).

2.8. Differentiation assay

ADSCs were characterized based on their adipogenic, osteogenic, and chondrogenic capacities. For the adipogenesis assay, the medium was changed to MSCgo adipogenic (Cosmobio, Tokyo, Japan). After 21 days, the cells were fixed with 4% paraformaldehyde (Muto Pure Chemical, Tokyo, Japan) for 1 h and stained with fresh oil red O solution (Fujifilm Wako Pure Chemical Corporation, Osaka, Japan) for 3 h. For the osteogenesis assay, the medium was switched to MSCgo Osteogenic (Cosmobio, Tokyo, Japan). After 21 days, the cells were stained with 1% alizarin red S solution (Wako Pure Chemical Industries, Osaka, Japan). For the chondrogenic assay, the medium was switched to MSCgo chondrogenic (Cosmobio, Tokyo, Japan). After 21 days, the cells were stained with 0.2 mL of 1% Alcian Blue solution (Wako Pure Chemical Industries, Osaka, Japan).

2.9. Fabrication of cell sheets using cryopreservation of ADSCs

ADSCs at passage 3 were harvested using trypsin–EDTA. The cells were suspended in CELLBANKER1 cryopreservation medium (3×10^6 cells in 1 mL; Zenoaq, Fukushima, Japan) and cryopreserved at −190 °C (MVE 800 series −190; MVE Cryosystems Japan Co., Tokyo, Japan). After cryopreservation for 1–10 months, the cells were immediately diluted in 10 mL DMEM and cultured in DMEM containing 10% FBS and 1% penicillin/streptomycin at 37 °C in a 5% CO_2 atmosphere. The cells were passaged every 3 days using trypsin–EDTA. The cells isolated at passage 5 were seeded on temperature-responsive cell culture dishes (35 mm diameter, UpCell, Cell Seed, Tokyo, Japan) at a density of 1×10^5 cells/dish. The cells were cultured in DMEM containing 10% FBS and 1% penicillin/streptomycin with 82 μg/mL ascorbic acid (Wako Pure Chemical Industry, Osaka, Japan) for 2 days. ADSC sheets were harvested by reducing the temperature from 37 °C to less than 32 °C for 30 min. The medium was removed to produce ADSC sheets.

2.10. ADSC sheet transplantation model in rabbits

The effect of bone hyperplasia was investigated in rabbits by removing the left maxillary mucosa and transplanting the ADSC sheet. The right maxillary sinus was the sham side, and only the maxillary mucosa was removed. The maxillary mucosa was removed using the same procedure as that in the nasal mucosa-removal model. ADSC sheets were washed twice with saline and aspirated with a 1 mL syringe, and transplanted at the maxillary sinus. Location was adjusted with forceps. After 4 weeks, the rabbits were sacrificed and evaluated using the same method as that in the nasal mucosa-removal model. Four SPF rabbits were used for experimentation.

2.11. Statistical analysis

Data analysis was performed using JMP Pro 12.0.0 (SAS, Cary, NC, USA). All values are presented as mean ± standard error of the mean (SEM). The Wilcoxon test was used to compare the two groups. $P < 0.05$ was considered statistically significant.

3. Results

3.1. Development of the nasal mucosa-removal model in rabbits

Three control samples, which were non-SPF rabbits, were evaluated at 4 weeks; and seven nasal mucosal-removal samples, four of which were SPF rabbits and three were non-SPF rabbits, were evaluated at 4 weeks (Table 1). At 4 weeks, three samples, which were non-SPF rabbits, were evaluated on the control side (right side) and mucosal removal side (left side) in the same animal. In six rabbits, the mucosa removal side in the nasal mucosa-removal model exhibited evident bone hyperplasia. The remaining samples only exhibited minor bone hyperplasia. A similar study was performed with evaluation of the control side (right side) and mucosa-removal side (left side) in the same animal on long-term models of non-SPF rabbits (one rabbit at 5 weeks, one rabbit at 7 weeks, one rabbit at 8 weeks, and two rabbits at 9 weeks). Three non-SPF rabbits in the nasal mucosa-removal long-term model exhibited purulent nasal discharge and infected nasal cavities on the control side. All short-term models were SPF rabbits (Table 1). None of the rabbits demonstrated any significant complications, including weight loss, throughout experimentation.

3.2. Nasal mucosa-removal model in rabbits

The results of the nasal mucosa-removal model in a rabbit at 4 weeks are shown in Figs. 2 and 3. Micro-CT findings revealed significant bone hyperplasia on the mucosa removal side and no bone hyperplasia on the control sham side (Fig. 2b–e). Bone hyperplasia was more prominent in the anterior part of the maxillary sinus than in the posterior region, and more pronounced in the maxillary sinus bone than in the nasal bone. The maxillary sinus bone area was compared between the control side at 4 weeks and the nasal mucosa removal side at 4 weeks (Fig. 2f). A significant difference was observed between the maxillary sinus bone areas on the control side and those on the removal side at 4 weeks (p-values for the anterior, middle, and posterior sections were 0.017, 0.030, and 0.030, respectively). Similar results were obtained in the two long-term rabbit models without intranasal infection. No significant difference was observed between the maxillary sinus bone areas on the control side and those on the mucosa-removal side in the three long-term models with intranasal infection (p-values for the anterior, middle, and posterior sections were 0.127, 0.275, and 0.513, respectively) (Fig. 2g). The results of tissue staining at 4 weeks are shown for the control in Fig. 3a, c and for the nasal mucosa removal sides in Fig. 3b, d. HE staining revealed fence-shaped bone tissue in the maxillary sinus mucosa removed at 4 weeks (Fig. 3a and b). Although the original maxillary sinus bone shape on the control side was preserved, that on the mucosa removal side was destroyed. Pan-cytokeratin immunostaining revealed epithelium in the maxillary sinus on the control side but not on the mucosa removal side (Fig. 3c and d). The nasal mucosa-removal model in a rabbit at 1, 3, 7, and 14 days is shown in Fig. 3e–h. Micro-CT findings revealed a low-density area in the maxillary sinus on days 1 and 3. The maxillary sinus was of fully low-density on day 7. A high-density area was present in the maxillary sinus on day 14 (Fig. 3e). On days 1 and 3, red blood cells were observed in the maxillary sinus (Fig. 3f). On day 7, a large amount of mesenchymal cell migration was observed in the exposed bone tissue of the maxillary sinus. In addition, the original maxillary sinus bone shape was preserved (Fig. 3f, h). On day 14,

Table 1
The nasal mucosa-removal model in a rabbit model.

	n
Control side 4 weeks	3
Nasal mucosal removal side 4 weeks	7
Nasal mucosal removal side 1 day	2
Nasal mucosal removal side 3 days	2
Nasal mucosal removal side 5 days	2
Nasal mucosal removal side 7 days	6
Nasal mucosal removal side 14 days	4

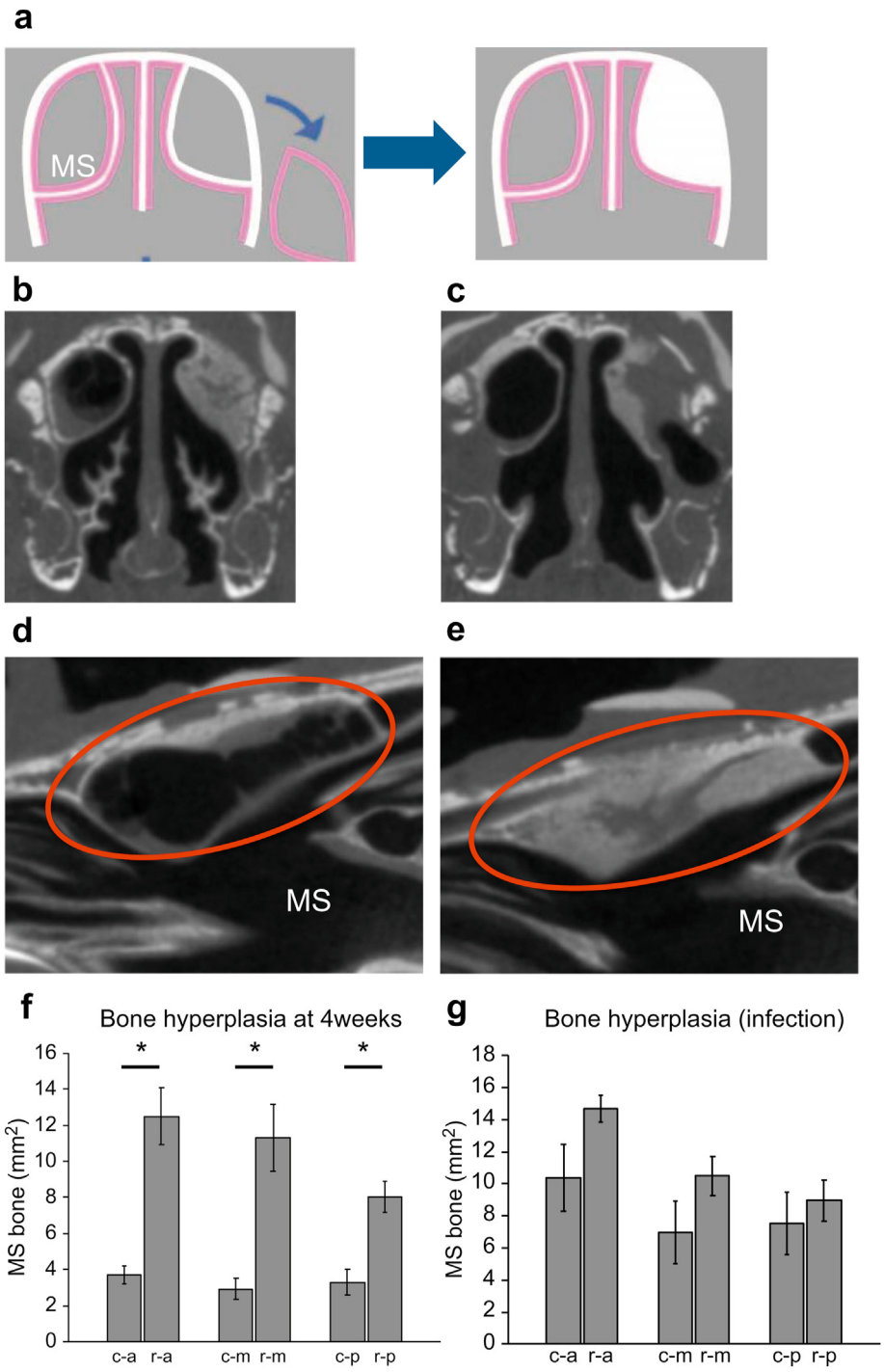

Fig. 2. A rabbit model 4 weeks after nasal mucosal removal. The rabbit's right side is the sham model, and the left side is the nasal mucosa removal side. (a) The schema for the nasal mucosa-removal model (b, c) Micro-computed tomography (micro-CT) imaging 4 weeks after nasal mucosa removal in the left maxillary sinus (MS), and simultaneously in the right side (control sham side). Anterior (b) and posterior (c) sections. CT imaging in the MS of the control sham side (d) and mucosa removal model side in sagittal sections (e). Micro-CT findings demonstrated significant bone hyperplasia only in the left MS. (f) Comparison of MS bone area (MS bone) between the control side at 4 weeks and the nasal mucosa removal side at 4 weeks. The data are presented as mean ± standard error of the mean. Average MS bone area was 3.7 mm^2 in control side anterior sections (c–a), 12.5 mm^2 in removal side anterior sections (r–a), 2.9 mm^2 in control side middle sections (c–m), 11.3 mm^2 in removal side middle sections (r–m), 3.3 mm^2 in control side posterior sections (c–p), and 8.0 mm^2 in removal side posterior sections (r–p). (g) Comparison of MS bone area between the control side and the nasal mucosa removal side with intranasal infection. Average MS bone area was 10.4 mm^2 in control side anterior sections (c–a), 14.7 mm^2 in removal side anterior sections (r–a), 7.0 mm^2 in control side middle sections (c–m), 10.5 mm^2 in removal side middle sections (r–m), 7.5 mm^2 in control side posterior sections (c–p), and 9.0 mm^2 in removal side posterior sections (r–p). *P < 0.05.

bone tissue was observed in the maxillary sinus, although the original maxillary sinus bone shape was destroyed (Fig. 3f). Pan-cytokeratin immunostaining revealed the absence of epithelial cells in the maxillary sinus on the mucosa removal side on days 1, 3, 7, and 14 (Fig. 3g).

3.3. Characterization of ADSCs and ADSC sheets

Spindle cells were observed in phase contrast microscope imaging for ADSCs at passage 5 (Supplementary Fig. S1a). ADSCs stained positively for CD44, but negatively for CD73, CD90, CD31,

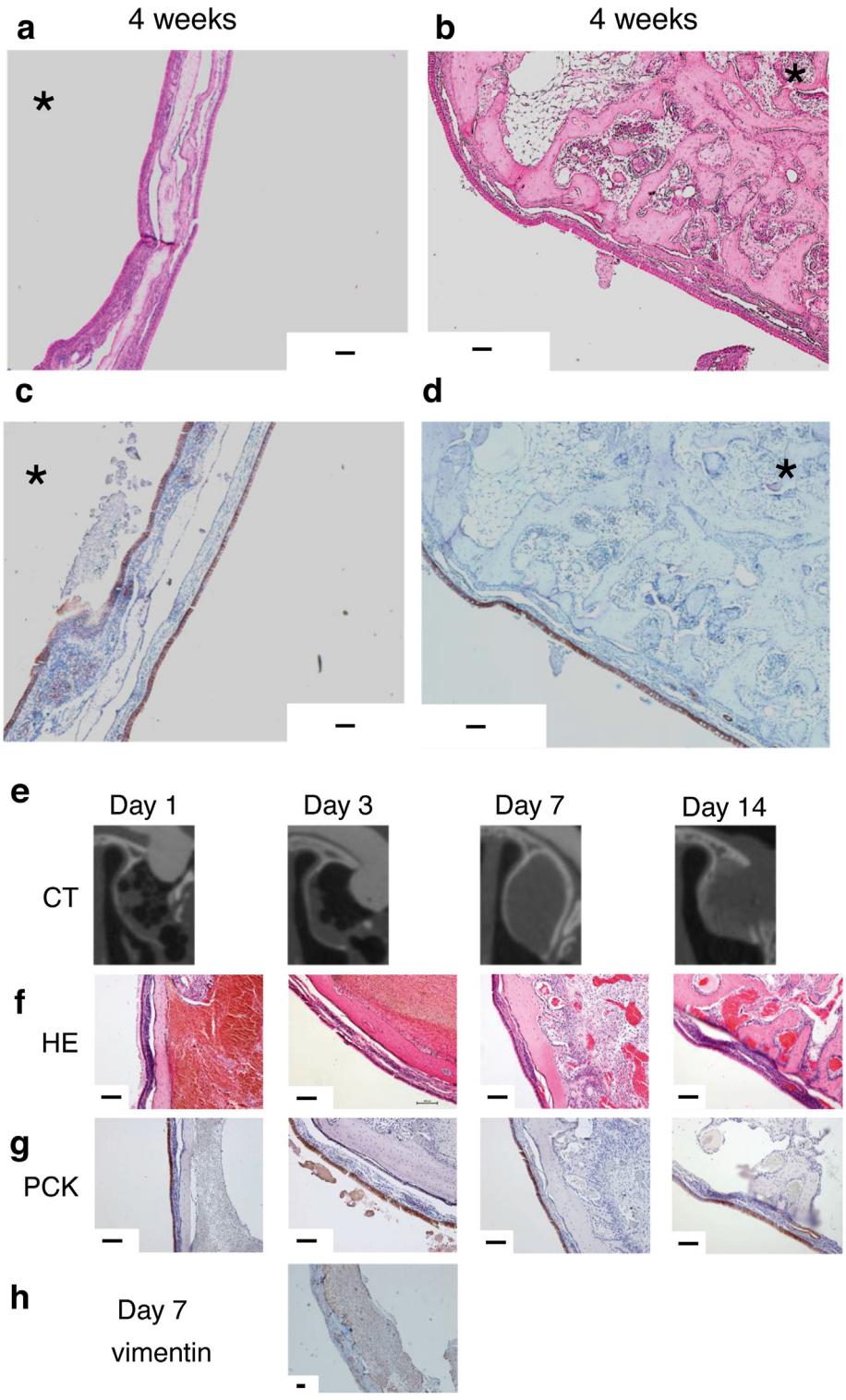

Fig. 3. Tissue staining at week 4. Micro-CT findings and tissue staining at days 1, 3, 7, and 14. Hematoxylin and eosin (HE) staining of control sham side (a) and mucosa removal side (b) in the maxillary sinus (c, d) Pan-cytokeratin immunostaining of control sham side (c) and mucosa removal side (d) in the maxillary sinus. Black asterisk indicates the maxillary sinus area (e–g) The nasal mucosa-removal model in rabbits on days 1, 3, 7, and 14. (e) Computed tomography (CT) imaging of coronal sections. (f) HE staining of coronal sections. (g) Pan-cytokeratin (PCK) immunostaining. (h) Vimentin immunostaining on day 7. Scale bar, 100 μm.

CD34, and CD45 (Supplementary Fig. S1b). Oil red O, alizarin red S, and Alcian Blue solution staining were used to evaluate the characteristics of the ADSCs. The ADSCs formed colonies and demonstrated adipogenic, osteogenic, and chondrogenic capabilities based on oil red O, alizarin red S, and AlcianBlue solution staining (Supplementary Fig. S1c). HE staining revealed 1–2 layers of cells (Supplementary Fig. S1d). ADSC sheets were harvested by reducing the temperature from 37 °C to less than 32 °C for 30 min (Fig. 4e).

3.4. ADSC cell sheet transplantation model in rabbits

The effect of bone hyperplasia was investigated in rabbits by removing the left maxillary mucosa and transplanting the ADSC sheet (Fig. 4a). The ADSC sheet was transferable by the method described above (Fig. 4b–d). The results of the ADSC cell sheet transplantation model in rabbits at 4 weeks are shown in Fig. 5. Micro-CT imaging demonstrated that bone hyperplasia on the transplantation side was suppressed compared to that on the sham side (Fig. 5a–d). HE staining revealed fence-shaped bone tissue in both maxillary sinuses. The entire interior of the maxillary sinus on the transplantation side did not exhibit bone hyperplasia (Fig. 5e). We compared the maxillary sinus bone area between the nasal mucosa removal side and that on the ADSC cell transplantation side at 4 weeks (Fig. 5f). No significant difference was observed between the nasal mucosa removal maxillary sinus bone area and ADSC cell transplantation maxillary sinus bone area across all sections.

4. Discussion

In this study, we developed an animal model of bone hyperplasia in the maxillary sinus. In rabbit models, we approached the maxillary sinus from the nasal bone side and removed the nasal mucosa without destroying the structures in the nasal cavity. We observed that bone hyperplasia occurred only in the models with nasal mucosa-removal; these findings suggest that the presence or absence of nasal mucosa has a significant effect on bone remodeling. Cell sheet transplantation, one of the options for nasal mucosa regeneration, was possible.

Relapse of sinusitis occurs with bone exposure after endoscopic endonasal surgery and bone hyperplasia. Although symptoms depend on the location of bone hyperplasia, rhinosinusitis recurs when bone hyperplasia occurs in the drainage pathway (especially in the frontal sinus drainage pathway) [7]. Treatments to prevent bone hyperplasia are crucial and depend on the development of robust animal models. The preparation of the animal model reported herein is easy and highly reproducible. It does not require special instruments or drugs and is useful as a model of intra-nasal bone hyperplasia. This animal model may permit the modulation of the wound healing response by intervening with local administration of drugs or local insertion of cells and materials.

Clinically, it is well established that bone hyperplasia occurs at the exposed bone surface in the nasal cavity after endoscopic sinus surgery because of poor nasal mucosa regeneration. However, there is a paucity of basic studies on bone hyperplasia in the nasal cavity in the field of otolaryngology, in which, bone hyperplasia in the maxillary sinus after Caldwell-Luc operation is known to occur [15, 16, 17]. Briefly, the procedure involves removal of the maxillary sinus mucosa by approaching the root of the tooth into the maxillary sinus. Bone hyperplasia in the maxillary sinus has been studied extensively in the dental field with sinus floor elevation [11, 12, 13]. In the case of implant placement in the maxillary sinus, if there is no distance to the maxillary sinus, it is necessary to raise the maxillary sinus mucosa to cause bone hyperplasia in the area of raised mucosa. In the field of dentistry, the maxillary sinus mucosa is termed the Schneider's membrane and must be preserved to perform sinus floor elevation. These phenomena indicate that the nasal mucosa is also important for preventing bone hyperplasia. Extensive research has attempted to enhance bone hyperplasia while preserving the maxillary sinus mucosa [18, 19, 20, 21]. Many studies have examined animal models of maxillary sinus bone hyperplasia while preserving maxillary sinus mucosa [22,23]. Nevertheless, an animal model that removes the maxillary sinus mucosa and causes maxillary sinus bone hyperplasia is lacking to date.

In a rabbit model, the site of nasal mucosa removal is the maxillary sinus because this structure can be evaluated using micro-CT, and the nasal mucosa in the maxillary sinus can be removed by surgical operation. This method does not injure the common nasal meatus, which is important for nose-breathing rabbits and is considered to have minimal deleterious effects on the animal. In this model, the anterior and superior maxillary mucosa were removed. It is impossible to remove the entire maxillary sinus mucosa due to substantial expansion of the maxillary sinus posteriorly and inferiorly. Since the posterior and inferior maxillary sinus mucosa remains intact, migration of the mucosa may affect the mucosa removal area. The nasal bone is opened, and the nasal mucosa is not removed on the sham side. The purpose of the sham side is to exclude the effects of nasal osteotomy and evaluate the effects of maxillary sinus mucosal removal on bone hyperplasia in isolation. The hall of the nasal bone is covered by silicone to prevent infections from external sources.

Micro-CT imaging revealed bone hyperplasia on the mucosa removal side on postoperative day (POD) 28. In contrast, bone hyperplasia did not occur on the sham side. The nasal mucosa is considered important for bone remodeling. Bone hyperplasia may not occur at all sites of nasal mucosa removal. Significant bone hyperplasia was observed in the anterior section of the maxillary sinus when compared to the posterior section. A possible reason for less bone hyperplasia in the posterior section is that the remaining normal posterior and inferior mucosa migrated to the site of nasal mucosa removal. The same results were obtained for models evaluated on the control side (right side) and mucosa removal side (left side) in the same animal. These results suggest that no contralateral bone hyperplasia effects occurred. HE staining and pan-cytokeratin immunostaining demonstrated that the maxillary sinus mucosa was preserved on the control side, suggesting that nasal osteotomy does not affect the maxillary sinus mucosa. The original shape of the maxillary sinus on the control side was preserved, suggesting that bone remodeling did not occur. HE staining and pan-cytokeratin immunostaining demonstrated fence-shaped bone tissue on the mucosa removal side, and the maxillary sinus mucosa was absent. Migration of the remaining mucosa did not suppress all maxillary sinus bone hyperplasia. The original shape of the maxillary sinus bone was destroyed, and bone remodeling has occurred. Osteoblast activation and osteoclast function may be simultaneously activated, but further studies are needed to prove this mechanism. Three non-SPF rabbits in the nasal mucosa removal model exhibited intranasal infections. A previous report demonstrated a high rate of *Pasteurella multilocida* infection in non-SPF rabbits when the respiratory epithelium was injured [24]. Minor bone hyperplasia was observed in the maxillary sinuses on the control side of intranasal infection rabbits, suggesting that intranasal infection caused bone hyperplasia. However, significant bone hyperplasia did not occur despite nasal cavity infection because the maxillary sinus mucosa on the control side was preserved. This study demonstrates that bone hyperplasia occurred only upon removing the nasal mucosa. The presence or absence of nasal mucosa was observed to have a significant effect on bone remodeling.

The process of bone hyperplasia is observed over a short period of time, and it is clear that several phases exist during this process. Red blood cell migration is observed early after surgery, followed by mesenchymal cell migration. Mesenchymal cells proliferated on POD 7 and differentiated into bone tissue on POD 14. The original maxillary sinus bone was preserved until POD 7 but was destroyed on POD 14. Fence-shaped bone tissue was observed on POD 28. Bone remodeling was observed on POD 14 and was completed by POD 28. Two types of osteogenesis exist: intramembranous osteogenesis and endochondral osteogenesis. Cartilage tissue was

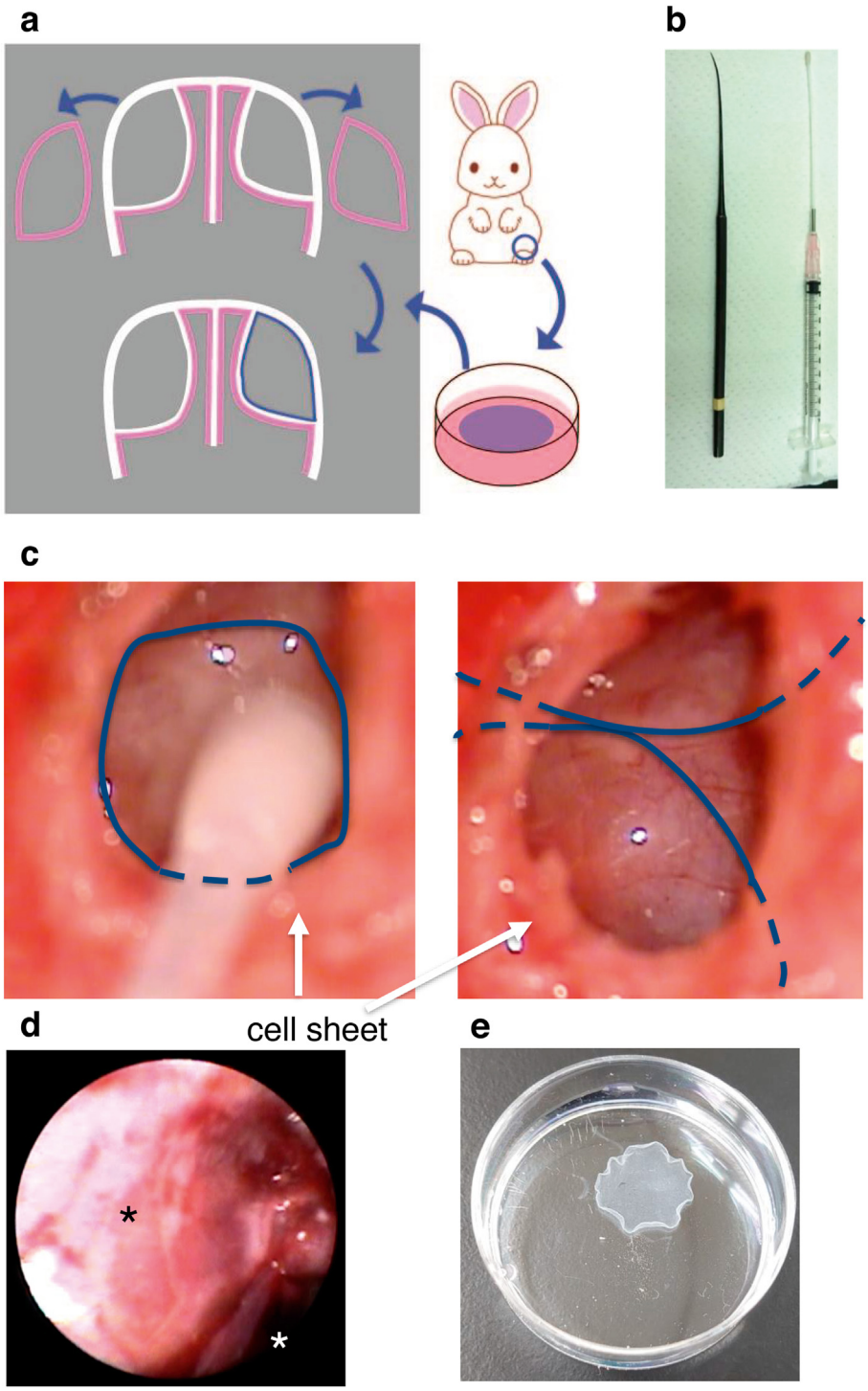

Fig. 4. The adipose-derived mesenchymal stromal cell sheet transplantation model in rabbits. (a) The schema for the cell sheet transplantation model. (b) Surgical instruments (c, d) Operative methods. (c) Microscope images. (d) Endoscopic view depicting the maxillary sinus. White and black asterisks indicate the presence of normal nasal mucosa and the transplantation area, respectively. (e) Adipose-derived mesenchymal stromal cell sheet.

not observed in these processes. Bone hyperplasia of the maxillary sinus is considered to occur due to intramembranous ossification [25]. These processes are similar to intramembranous bone healing subsequent to tooth extraction [9].

Cell sheets fabricated by temperature-responsive culture dishes have been applied to various tissue reconstructions such as corneal dysfunction [26], myocardial infarction [27], esophageal ulcerations [28], diabetic ulcers [29], and periodontitis [30]. Cell sheets using temperature-responsive cell culture dishes can be collected in sheet form with adhesive factors present [31]. Moreover, the remaining adhesion factors facilitate transplantation of cells to the target site. We have successfully regenerated the middle ear mucosa by transplanting autologous nasal mucosal epithelial cell sheets onto exposed the middle ear bone surface [7]. We thought

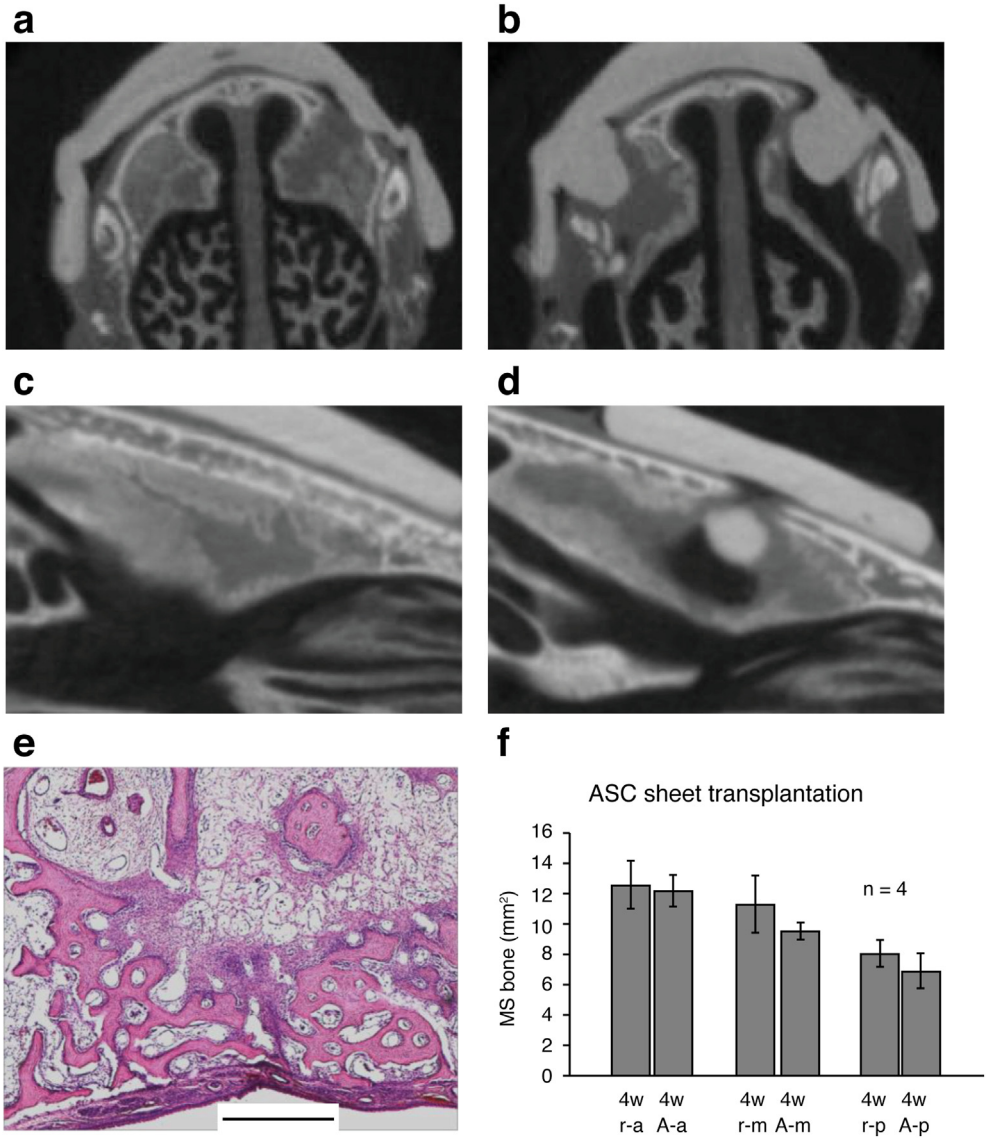

Fig. 5. A rabbit model 4 weeks after transplantation of the adipose-derived mesenchymal stromal cell (ADSC) sheet. The rabbit's right side is the nasal mucosa removal side, and the left side is the cell sheet transplantation side (c, e) Control side (d, f) Cell sheet transplantation side (a, b) Micro-computed tomography (micro-CT) imaging of coronal sections. (a) Anterior section. (b) Posterior section (c, d) CT imaging of the maxillary sinus in sagittal sections. Bone hyperplasia of the transplantation side is suppressed compared to that on the sham side. (e) Hematoxylin and eosin staining. Cells resembling white adipocytes are observed in the maxillary sinus of the transplantation side. Scale bar, 500 μm. (f) Comparison of maxillary sinus bone area (MS bone) at 4 weeks between the nasal mucosa removal side and ADSC transplantation side. The data are presented as mean ± standard error of the mean. Average maxillary sinus bone area was 12.5 mm^2 in removal side anterior sections (r–a), 12.0 mm^2 in ADSC cell transplantation side anterior sections (A–a), 11.3 mm^2 in removal side middle sections (r–m), 9.5 mm^2 in ADSC transplantation side middle sections (A-m), 8.0 mm^2 in removal side posterior sections (r–p), and 6.9 mm^2 in ADSC transplantation side posterior sections (A-p).

that regeneration of the nasal mucosa could be expected by covering the exposed nasal bone surface with cultured cells. Although cell sheets have a significant advantage in terms of covering a large area of the defect, maintaining their shape during implantation is difficult, and they cannot be grasped with forceps. Further, transplantation is technically demanding. The mucosal removal model in this study allowed an easy approach to the maxillary sinus and cell sheet transplantation with a good field of view.

Nasal mucosal epithelial cell sheets may be a good source of cell sheets that inhibit bone hyperplasia [7]. Nasal mucosal cell sheets are best used as autologous transplants from an immunological point of view. It is possible to harvest nasal mucosal epithelium using methods described in previous papers; however, these approaches would damage the maxillary sinus and affect the experimental results of this study, which were analyzed in the nasal cavity [7]. It is difficult to harvest the nasal mucosa without damaging the maxillary sinus. In this study, we used ADSCs as the source of the cell sheets, which can be collected without manipulation of the nasal cavity. In this study, ADSC sheets could be implanted. ADSC sheet transplantation was able to cover all mucosal removal sites. No significant differences in bone hyperplasia were found between the transplantation side and the sham side in terms of the effect of transplantation of the ADSC sheet, however, there was a tendency to inhibit bone hyperplasia in the area near the remaining nasal mucosa. In the posterior part of the

maxillary sinus, ADSCs served as a scaffold to facilitate migration of the remaining nasal mucosa, which may have inhibited bone hyperplasia. In the future, the source of cell sheets should be changed and a more appropriate cell source for mucosal regeneration should be considered. The ADSCs used in this study may have lacked stem cell properties. The surface markers CD73 and CD90, which are present in mesenchymal stem cells, were not expressed in the ADSCs in this experiment. ADSCs did not differentiate into adipocytes. If the potential of ADSCs was sufficient, a better therapeutic effect might have been achieved.

In this study, we created a clinically relevant model of epithelial mucosal detachment and investigated the effects of cell sheet transplantation. Although the implantation of ADSC sheets showed some effect, more effective methods of cell therapy would need to be considered.

5. Conclusions

This model could be useful as a pathological model because it has applicability in various therapeutic interventions. The presence or absence of the nasal mucosa affects bone remodeling, which highlights the importance of regeneration of the nasal mucosa. In nasal mucosal regeneration therapy, the ADSC sheet had an inhibitory effect on bone hyperplasia. Cell therapy is expected to regenerate the nasal mucosa.

Declaration of competing interest

Co-author Masayuki Yamato is an equity holder of CellSeed Inc.; Tokyo Women's Medical University currently receives research funding from CellSeed, Inc. Dr. M. Yamato is also an advisor of commercial efforts, Helios, and NIPPI (Japan).

Acknowledgments

This work was supported by JSPS KAKENHI [Grant Number JP19k188784] and Jikei University Strategic Prioritizing Research fund, and was partly supported by Institute of Laboratory Animals (ILA), Tokyo Women's Medical University.

Appendix A. Supplementary data

Supplementary data related to this article can be found at https://doi.org/10.1016/j.reth.2020.12.004.

References

[1] Gross WE, Gross CW, Becker D, Moore D, Phillips D. Modified transnasal endoscopic Lothrop procedure as an alternative to frontal sinus obliteration. Otolaryngol Head Neck Surg 1995;113:427–34.
[2] Anderson P, Sindwani R. Safety and efficacy of the endoscopic modified Lothrop procedure: a systematic review and meta-analysis. Laryngoscope 2009;119:1828–33.
[3] Shih LC, Patel VS, Choby GW, Nakayama T, Hwang PH. Evolution of the endoscopic modified Lothrop procedure: a systematic review and meta-analysis. Laryngoscope 2018;128:317–26.
[4] Papay FA, Maggiano H, Dominquez S, Hassenbusch SJ, Levine HL, Lavertu P. Rigid endoscopic repair of paranasal sinus cerebrospinal fluid fistulas. Laryngoscope 1989;99:1195–201.
[5] Jho HD, Carrau RL. Endoscopic endonasal transsphenoidal surgery: experience with 50 patients. J Neurosurg 1997;87:44–51.
[6] Wang EW, Zanation AM, Gardner PA, Schwartz TH, Eloy JA, Adappa ND, et al. ICAR: endoscopic skull-base surgery. Int Forum Allergy Rhinol 2019;9:S145–365.
[7] Yamamoto K, Hama T, Yamato M, Uchimizu H, Sugiyama H, Takagi R, et al. The effect of transplantation of nasal mucosal epithelial cell sheets after middle ear surgery in a rabbit model. Biomaterials 2015;42:87–93.
[8] Yamamoto K, Yamato M, Morino T, Sugiyama H, Takagi R, Yaguchi Y, et al. Middle ear mucosal regeneration by tissue-engineered cell sheet transplantation. NPJ Regen Med 2017;2:6.
[9] Vieira AE, Repeke CE, Ferreira Junior Sde B, Colavite PM, Biguetti CC, Oliveira RC, et al. Intramembranous bone healing process subsequent to tooth extraction in mice: micro-computed tomography, histomorphometric and molecular characterization. PLoS One 2015;10:e0128021.
[10] Boyne PJ, Herford AS. Distraction osteogenesis of the nasal and antral osseous floor to enhance alveolar height. J Oral Maxillofac Surg 2004;62:123–30.
[11] Jensen J, Simonsen EK, Sindet-Pedersen S. Reconstruction of the severely resorbed maxilla with bone grafting and osseointegrated implants: a preliminary report. J Oral Maxillofac Surg 1990;48:27–33.
[12] Raja SV. Management of the posterior maxilla with sinus lift: review of techniques. J Oral Maxillofac Surg 2009;67:1730–4.
[13] Sullivan SM, Bulard RA, Meaders R, Patterson MK. The use of fibrin adhesive in sinus lift procedures. Oral Surg Oral Med Oral Pathol Oral Radiol Endod 1997;84:616–9.
[14] Yoshimura H, Muneta T, Nimura A, Yokoyama A, Koga H, Sekiya I. Comparison of rat mesenchymal stem cells derived from bone marrow, synovium, periosteum, adipose tissue, and muscle. Cell Tissue Res 2007;327:449–62.
[15] Barzilai G, Greenberg E, Uri N. Indications for the Caldwell-Luc approach in the endoscopic era. Otolaryngol Head Neck Surg 2005;132:219–20.
[16] Matheny KE, Duncavage JA. Contemporary indications for the Caldwell-Luc procedure. Curr Opin Otolaryngol Head Neck Surg 2003;11:23–6.
[17] Tange RA. Some historical aspects of the surgical treatment of the infected maxillary sinus. Rhinology 1991;29:155–62.
[18] Pikos MA. Maxillary sinus membrane repair: report of a technique for large perforations. Implant Dent 1999;8:29–34.
[19] Proussaefs P, Lozada J, Kim J. Effects of sealing the perforated sinus membrane with a resorbable collagen membrane: a pilot study in humans. J Oral Implantol 2003;29:235–41.
[20] Testori T, Wallace SS, Del Fabbro M, Taschieri S, Trisi P, Capelli M, et al. Repair of large sinus membrane perforations using stabilized collagen barrier membranes: surgical techniques with histologic and radiographic evidence of success. Int J Periodontics Restor Dent 2008;28:9–17.
[21] Kim YK, Yun PY, Oh JS, Kim SG. Prognosis of closure of large sinus membrane perforations using pedicled buccal fat pads and a resorbable collagen membrane: case series study. J Korean Assoc Oral Maxillofac Surg 2014;40:188–94.
[22] Iida T, Carneiro Martins Neto E, Botticelli D, Apaza Alccayhuaman KA, Lang NP, Xavier SP. Influence of a collagen membrane positioned subjacent the sinus mucosa following the elevation of the maxillary sinus. A histomorphometric study in rabbits. Clin Oral Implants Res 2017;28:1567–76.
[23] Lim HC, Son Y, Hong JY, Shin SI, Jung UW, Chung JH. Sinus floor elevation in sites with a perforated schneiderian membrane: what is the effect of placing a collagen membrane in a rabbit model? Clin Oral Implants Res 2018;29:1202–11.
[24] Morino T, Kikuchi S, Inagaki T, Komori M, Yamamoto K, Kojima H, et al. Lessons learned from conventional animals: encouragement to use specific-pathogen-free animals. Regen Ther 2020;14:296–8.
[25] Scott CK, Hightower JA. The matrix of endochondral bone differs from the matrix of intramembranous bone. Calcif Tissue Int 1991;49:349–54.
[26] Nishida K, Yamato M, Hayashida Y, Watanabe K, Yamamoto K, Adachi E, et al. Corneal reconstruction with tissue-engineered cell sheets composed of autologous oral mucosal epithelium. N Engl J Med 2004;351:1187–96.
[27] Miyahara Y, Nagaya N, Kataoka M, Yanagawa B, Tanaka K, Hao H, et al. Monolayered mesenchymal stem cells repair scarred myocardium after myocardial infarction. Nat Med 2006;12:459–65.
[28] Ohki T, Yamato M, Murakami D, Takagi R, Yang J, Namiki H, et al. Treatment of oesophageal ulcerations using endoscopic transplantation of tissue-engineered autologous oral mucosal epithelial cell sheets in a canine model. Gut 2006;55:1704–10.
[29] Kato Y, Iwata T, Morikawa S, Yamato M, Okano T, Uchigata Y. Allogeneic transplantation of an adipose-derived stem cell sheet combined with artificial skin accelerates wound healing in a rat wound model of type 2 diabetes and obesity. Diabetes 2015;64:2723–34.
[30] Iwata T, Yamato M, Tsuchioka H, Takagi R, Mukobata S, Washio K, et al. Periodontal regeneration with multi-layered periodontal ligament-derived cell sheets in a canine model. Biomaterials 2009;30:2716–23.
[31] Yamato M, Utsumi M, Kushida A, Konno C, Kikuchi A, Okano T. Thermo-responsive culture dishes allow the intact harvest of multilayered keratinocyte sheets without dispase by reducing temperature. Tissue Eng 2001;7:473–80.